Graph-Based Risk Assessment and Error Detection in Radiation Therapy

Reshma Munbodh[1], Juliana K. Bowles[2] and Hitten P. Zaveri[3]

[1] Department of Radiation Oncology, Alpert Medical School of Brown University, Providence, RI 02903, USA

[2] School of Computer Science, University of St Andrews, Fife, St Andrews KY19 9SX, UK

[3] Department of Neurology, Yale University, New Haven, CT 06511, USA

Reshma Munbodh, Ph.D.
Department of Radiation Oncology
Alpert Medical School of Brown University
593 Eddy Street
Providence, RI 02903
Reshma_Munbodh@brown.edu
+1-401-444-5245

This article has been accepted for publication and undergone full peer review but has not been through the copyediting, typesetting, pagination and proofreading process, which may lead to differences between this version and the Version of Record. Please cite this article as doi: 10.1002/MP.14666

Abstract. Purpose: The objective of this study was to formalize and automate quality assurance (QA) in radiation oncology. QA in radiation oncology entails a multistep verification of complex, personalized radiation plans to treat cancer involving an interdisciplinary team and high technology, multivendor software and hardware. We addressed the pretreatment physics chart review (TPCR) using methods from graph theory and constraint programming to study the effect of dependencies between variables and automatically identify logical inconsistencies and how they propagate.

Materials and Methods: We used a modular approach to decompose the TPCR process into tractable units comprising subprocesses, modules and variables. Modules represent the main software entities comprised in the radiation treatment planning workflow and subprocesses group the checks to be performed by functionality. Module-associated variables serve as inputs to the subprocesses. Relationships between variables were modeled by means of a directed graph. The detection of errors, in the form of inconsistencies, was formalized as a constraint satisfaction problem whereby checks were encoded as logical formulae. The sequence in which subprocesses are visited was described in a activity diagram.

Results: The comprehensive model for the TPCR process comprised 5 modules, 19 subprocesses and 346 variables, 225 of which were distinct. Modules included "Treatment Planning System" and "Record and Verify System". Subprocesses included "Dose Prescription", "Documents", "CT Integrity", "Anatomical Contours", "Beam Configuration", "Dose Calculation", "3D Dose Distribution Quality" and "Treatment Approval". Variable inconsistencies, their source and propagation are determined by checking for constraint violation and through graph traversal. Impact scores, obtained through graph traversal, combined with severity scores associated with an inconsistency, allow risk assessment.

Conclusions: Directed graphs combined with constraint programming hold promise for formalizing complex QA processes in radiation oncology, performing risk assessment and automating the TPCR process. Though complex, the process is tractable.

Keywords: Graphs, automated checks, physics chart review, risk assessment, model

1 Introduction

More than 50% of patients diagnosed with cancer receive radiation therapy (RT). Radiation therapy involves the treatment of patients with ionizing radiation to eradicate cancer cells. Since radiation not only kills cancer cells, but also damages normal cells, potentially causing radiation-induced toxicity, the aim of RT is to maximize the radiation dose delivered to the tumor in order to achieve local control while minimizing irradiation of healthy tissue so as to minimize the risk of post-treatment complications.

In external beam radiation therapy (EBRT), a CT of the patient is first acquired, from which a highly conformal and complex patient-specific radiation treatment plan is created. The plan delivers a physician-prescribed radiation dose to the tumor subject to associated dosimetric constraints to organs at risk. During the treatment planning process, peer review is critical to ensure the quality of the radiation plan. The most important form of peer review is the pretreatment physics chart review (TPCR). This is an extensive and time-consuming review, which is typically performed by a qualified medical physicist as part of the approval process of the radiation plan for treatment. The TPCR aims to verify the safety and correctness of all aspects of the treatment chart from the documentation to the integrity of the CT used for treatment planning, the quality and safety of the planned treatment, completion of physician review of the plan, patient specific quality assurance (QA) and consistency among treatment plan parameters in the treatment planning and electronic medical record systems. Best practice recommends that radiation treatment should not start until this review is complete and the patient's treatment chart, including the radiation treatment plan, has been determined to be complete, safe and free of errors.

The TPCR, therefore, entails a multistep and comprehensive chart review. It requires interaction with an interdisciplinary team and the conduct of integrity and consistency checks of dozens of variables across multivendor and multifunction software and hardware systems. The medical physicist may have multiple charts to check simultaneously and they may be expected to perform the TPCR within a short time. A duration of thirty minutes to one hour per chart is not unusual. According to an all member survey

conducted by AAPM Task Group 275, 74.1% of participants reported checking up to five charts in a day, 17.7% from 6 to 10 charts and 8.2% more than 11 charts in one day [1].

A study by Gopan et al. [2] assessing the effectiveness of the TPCR found that most potentially detectable errors in the radiation therapy process originate at treatment planning, thus underscoring the importance of the TPCR in detecting errors prior to treatment and in ensuring treatment safety and efficacy. Moreover, they report that only 38% of potentially detectable events in the institutional departmental incident learning system were detected during the TPCR. A further review of the Safety in Radiation Oncology (SAFRON) [3] database of incidents that reached patients indicated that none of potentially detectable events in the patients' treatment charts were detected by the TPCR . The authors concluded that while the pretreatment physics chart review is one of the most effective quality control checks in radiation oncology, its effectiveness could be improved through standardization and automation.

The TPCR is frequently performed manually, with, according to the AAPM Task Group 275 survey, 47.9% of personnel in radiation oncology conducting a manual review, 47.4% a combination of manual and automated checks and approximately 4.7% using an automated chart review process [1]. Mazur et al. [4] reported that physicists have the highest workload among professionals in radiation oncology and are also subject to a high number of stressors. The combination of high workloads, large teams in busy clinics, increasingly complex radiation therapy techniques and a lack of standardization may unfortunately contribute to errors not being detected during the TPCR.

A key recommendation of AAPM Task Group 275, the objective of which was to provide recommendations on the physics chart review, is the development of automated tools to assist with the chart review task [1]. Most current automated and semi-automated chart review tools are similar to an automated checklist to verify the integrity of variables in a specific module or their consistency across software components used to create the treatment plan based on predefined rules [5, 6, 7, 8, 9, 10, 11, 12, 13, 14]. Several studies have shown the use of such tools to increase efficiency and patient safety and to reduce the rate of plan revisions, avoidable safety events and patient delays [10, 11, 13].

A limitation of these chart review tools is that they do not provide contextual information about errors and inconsistencies. Contextual information includes the source of potential errors and how they may propagate. It is important for risk assessment [15], which entails a combination of risk analysis and evaluation. In risk analysis, the cause, frequency and consequences of a hazardous event are assessed. Risk analysis contributes in part to risk evaluation, whereby the tolerability of a hazardous event, and, potentially, the urgency and sequence in which the event should be addressed is evaluated. Such contextual information may help capture the complexity of the TPCR and facilitate error detection and correction. Risk assessment of the TPCR process may also help with the implementation of clinical guidelines to reduce the risk of serious errors occurring during treatment planning.

We propose a chart review solution that incorporates information about the architecture and structure of the TPCR process by means of a directed graph that models relationships between variables [16]. The vertices of this graph represent variables in the TPCR process and edges model the relationships between variables. Through graph traversal, we determine the source of an error and how it propagates through the TPCR process. A quantitative assessment of the consequence of an error on other variables, described by an *impact* score, is obtained by recursively finding the successors of vertices connected to the inconsistent variable at all levels. The tolerability of an error, or its potential to cause harm to a patient, is described using a preassigned *severity* score. Thus, prior domain-based knowledge on the variables being checked in the form of information about how they are connected to other variables allows quantification of the cause of an error, its impact or consequence on other variables in the TPCR and its severity in terms of harm to the patient, and therefore its risk. We also briefly describe how information about the source of an error and how it propagates may be used for risk assessment.

We formalize the full TPCR process as a constraint satisfaction problem, whereby variables are allowed to take on values in their domain and checks are modeled as logical formulae describing variable constraints. We propose to detect inconsistencies by solving the formulae and checking for constraint violation. To implement a solution to our problem, we decompose the TPCR process into tractable units comprising,

modules, subprocesses and variables. The types and sequence of the checks to be performed are captured in the subprocesses and an activity diagram, respectively.

In Section 2, we describe how relationships between variables are represented. We describe how to model the TPCR as a directed graph and formulate the TPCR as a constraint satisfaction problem. In Section 3, we present the results of this study and in Section 4, we discuss the results in the context of other studies in the field. We present our conclusions in Section 5. Note that throughout the manuscript, the terms errors and inconsistencies is used interchangeably.

2 Materials and Methods

Fig. 1 illustrates the customary workflow for external beam radiation therapy (EBRT) planning and delivery. Prior to commencing radiation treatment, the physician enters a prescription for the radiation dose to be delivered to the patient. A 3D diagnostic energy CT scan of the patient is acquired by a therapist for treatment planning purposes. The CT gives accurate three-dimensional anatomical information about the patient's bony and soft tissue anatomy, enabling delineation of the target treatment volume and organs at risk. A dosimetrist then creates a patient-specific radiation treatment plan. Dosimetric constraints to the delineated anatomical structures are used, either directly or indirectly, in the calculation of the radiation dose distribution on the CT so that the desired prescribed dose is delivered to the target while sparing the organs at risk. The planned treatment is then reviewed for correctness and approved by the physician. Subsequently, a medical physicist performs the TPCR. If no errors or inconsistencies are detected in the treatment chart, the treatment plan is approved for treatment by the medical physicist. The planned treatment is then delivered to the patient on the treatment machine. Additional checks are performed to verify the correctness of the delivered dose. While this example illustrates the workflow in EBRT, it is generally applicable to other types of radiation therapy.

In the next sections, we introduced the notation used in this study. We describe how to decompose the TPCR process into its subcomponents, modeling the TPCR as a directed graph and the use of constraint satisfaction theory to detect errors during the TPCR.

2.1 Notation

The TPCR entails verifying the correctness and consistency of a number of items in a patient's treatment chart across various software modules. Let $\mathbf{M} = \{M_1, M_2, \ldots, M_m\}$ denote the software modules in the radiation therapy planning workflow. Modules include the document manager in the electronic medical record system, the treatment planning system, the record and verify system, independent monitor unit calculation software and intensity modulated radiation therapy (IMRT) QA software. The checks performed during the TPCR can be grouped into categories by functionality, which we refer to as subprocesses, while the items to be checked are encoded by variables. Let $\mathbf{P} = \{SP_1, SP_2, \ldots, SP_p\}$ denote the set of subprocesses comprising the TPCR process, P. $\mathbf{X} = \{X_1, X_2, \ldots, X_q\}$ denotes the set of individual items to be checked, for instance patient name and prescription dose. $\mathbf{V} = \{V_1, V_2, \ldots, V_n\}$ denotes the set of directly observable and latent variables representing all items to be checked. Here, $n > q$ since an item, X_i, for example, prescription dose, can appear in multiple modules, for example, the document manager, treatment planning system and record and verify modules. In this case, multiple variables, $\{V_j, V_{j+1}, \ldots, V_{j+k}\}$ will be associated with that item, each specific to the module in which the item appears and each representing a vertex in the graph of the TPCR as described in Section 2.3. A module, M_i, contains a unique subset of $\mathbf{V}$. A subprocess may contain variables from different modules.

In our notation, uppercase letters denote objects while lowercase letters denote observed values.

The steps necessary to formalize the TPCR process are displayed in Fig. 2. They include defining the relationships between variables, building and traversing a directed graph built from these relationships, and formulating a constraint satisfaction problem. These steps are described in more detail in the subsections below.

2.2 Variable Relationships

The next step in capturing the TPCR process is to define the relationships between variables. This enables determination of the source, impact and severity of an error. The types of relationships modeled are causal dependencies and conflicts. A variable is causally related to another variable if its occurrence contributes to the production of the value of the second variable. Mutually causal variables result in a cycle. A conflict exists between two variables if they are mutually exclusive, that is, the existence of one variable precludes the existence of the other.

The relationships between all variables in the TPCR process are captured in an adjacency matrix where entries in the first column define parent variables. A value of 0 in a cell indicates an absence of a relationship between two variables, a 1 indicates a causal relationship and a -1, a conflict.

2.3 Modeling the TPCR as a Directed Graph

The source of inconsistencies and how they propagate through the TPCR process, is identified using a directed graph built from the adjacency matrix.

The directed graph of the TPCR process is a pair $G = (\mathbf{V}, \mathbf{E})$, where $\mathbf{V}$ is a set of vertices and $\mathbf{E}$ is a set of edges. Here, $\mathbf{V} = \{V_i, \ldots, V_n\}$ is a set of vertices where each vertex, V_i, in the graph is directly mapped to the corresponding variable V_i. $\mathbf{E} = \{E_{ij}\} = \{(V_i, V_j), i \in \{1, \ldots, n\}, j \in \{1, \ldots, n\}, i \neq j\}$ is a set of directed edges, E_{ij}, where each element in the set is a tuple denoting an ordered pair of vertices. A directed edge, E_{ij} from vertices V_i to V_j, exists if V_j is dependent on V_i. If V_i is not related to any other variables, V_j is set to the empty set, ϕ.

In addition, we defined the following parameters on G. The indegree, λ_i^{in}, of variable V_i is defined as the number of edges going into the vertex V_i from its direct predecessor vertices and the outdegree, λ_i^{out} is defined as the number of edges originating from V_i to its direct successor vertices. The level of a vertex, V_j, with respect to V_i is determined by the shortest distance or minimum number of edges leading to V_j from V_i. The outconnection degree, ζ_i^{out}, of variable V_i is defined as the order of, or the number of vertices in

the subgraph obtained by recursively visiting the successor vertices (or children) of V_i, their successors and so on. Similarly, its inconnection degree, ζ_i^{in}, is the order of the subgraph obtained by recursively visiting all predecessor vertices (or parents) and their predecessors. In a similar fashion, we can find the number of edges going into or leaving vertex V_i at intermediate levels of connection.

2.4 Constraint Satisfaction Problem

The detection of errors and inconsistencies in the TPCR can be formalized as a constraint satisfaction problem. Given the finite set of variables $\mathbf{V} = \{V_1, \ldots, V_n\}$ with variable relationships described in Section 2.2, we define the following *c*onstraint network:

- A set of domains, $D = \{D_1, D_2, \ldots, D_n\}$, where $D_i = D(V_i)$ represents the set of values that variable V_i can take,
- A set of constraints, $C = \{C_1, C_2, \ldots, C_n\}$, where every constraint C_i is a pair $\langle V_i, R_i \rangle$. R_i defines the set of relations between all variables directly connected to V_i on the subset of domains.

If a variable is not related to any other variables, the constraint on that variable is defined by a unary constraint given by its domain.

We model three different types of constraints:

Extensional constraints: These are defined by enumerating the set of allowable simultaneous values for V_i. For instance, in the context of diagnosis and prescription dose, these are a set of tuples listing different diagnoses and associated prescription dose

Arithmetic constraints: These are defined by an arithmetic expression, using $=, \neq, <, >, \leq, \geq, \ldots$ on V_i. An examples is *prescription dose = dose per fraction × number of fractions*

Logical constraints: The constraints are defined using propositional or first order logic.

Constraint satisfaction is indicated by means of a Boolean function. An evaluation of the TPCR process is *consistent* and *complete* if all constraints are satisfied and the evaluation includes all variables.

2.5 Error Detection, Source and Propagation

The proposed steps in the automated chart review are shown in Fig. 3.

Evaluation of the TPCR process can either be performed simultaneously, that is, all errors and inconsistencies can be detected at once, or sequentially. For the sequential approach, the order in which the variables are checked is determined by an activity diagram describing the order in which the subprocesses in the TPCR are visited.

When a variable, V_i, is found to be inconsistent, the possible sources of the inconsistency at the first level are determined from the direct predecessor vertices of V_i. Possible sources of error at a deeper level can be found recursively in the same manner. The set of vertices so identified are called the parent vertices of V_i and the corresponding variables give all possible sources of inconsistency for V_i. The inconnection degree gives the total number of variables in the TPCR process that have a direct or indirect effect on V_i.

Similarly, the way in which an error or inconsistency propagates, or the set of all variables impacted by V_i is found recursively from the successor vertices of V_i. The variables so identified are called children of V_i. The outconnection degree gives the total number of variables directly or indirectly impacted by V_i.

The modular and graph-based approach employed allows ready determination of the software module and subprocess containing the inconsistency as well as the list of additional modules and subprocesses affected by the inconsistency.

The *severity* of an inconsistency is defined by a preassigned score influenced by domain knowledge and clinical experience. We define three levels of severity as follows: 0 is a warning that will not result in harm to the patient such as the use of a non-standard name for an organ at risk, 1 means that the inconsistency needs attention but the chart reviewer can proceed with the chart review or other error corrections simultaneously, 2 is a hard stop that may cause serious harm to a patient, for instance a wrong prescription dose or target contour, and needs immediate attention and correction. The *impact* score of a potential error on other variables, or how it propagates, is determined from its outconnection degree, ζ^{out}.

2.6 Risk Assessment

The combination of information obtained from the inconnection and outconnection analysis, impact and severity of an inconsistency is useful for risk analysis and evaluation. In risk analysis, the cause and likelihood of an adverse event occurring are assessed. Here, the potential cause of an inconsistency is obtained from the set of parent vertices at different levels of connection, λ^{in} and ζ^{in}. This information, combined with the probability of an error occurring in the parent variables, may be used to estimate the probability of the inconsistency or error occurring. In risk evaluation, the tolerability of the error is assessed. Here, information obtained from the inconnection and outconnection degrees along with preassigned severity scores can be used for risk evaluation. The priority in which an error or inconsistency is corrected may be partly determined from its severity, impact and the order of the subprocess to which it belongs relative to other subprocesses. For example, priority could be given to variables with high outconnection degree and which appear early in the subprocesses, since they impact many variables, and to variables with a high severity score. Other priority schemes based on the graph, subprocesses and modules can also be explored.

3 Results

The full model for the TPCR process comprised 5 modules, 19 subprocesses 225 distinct items (number of elements in $\mathbf{X}$) and 346 variables (number of elements in $\mathbf{V}$). The nomenclature used for the variables consisted of the name of the item being checked with the module name as suffix.

3.1 Modules

Modules, which define the software entities used in the treatment planning process, comprised the patient (document) manager, treatment planning system, record and verify system, independent MU calculation software and IMRT QA software.

3.2 Subprocesses

The subprocesses comprising the TPCR process and the logical flow in which they are linked is illustrated in the activity diagram shown in Fig. 4. The flow of sequential checks is determined by the relative order of the subprocesses.

Each subprocess describes a particular activity or feature of the TPCR process. In the full model, not illustrated here due to space considerations, the subprocesses are further subdivided into finer entities thus allowing a grouping of the checks at a finer granularity. In Fig. 4, "Patient Information and Plan Status" describes the checks associated with verifying that parameters describing the patient name and medical record number, treatment plan name, treatment course number and whether the treatment chart is ready to be reviewed. "Planning Intent and Dose Prescription" verifies that the radiation dose and treatment prescription information entered by the physician is correct and consistent across modules. "Presence of Primary Treatment Related Documents" verifies that all documents necessary for treatment planning, treatment delivery and documentation of the patients treatment plan are present in the treatment chart. "Image Integrity" verifies that the images present in the treatment planning system were acquired according to the physicians specifications. It also reviews the quality of the CT image including identifying the presence of artifacts. In "CT Internal Structures", the presence of contours delineating the anatomical structures listed in the planning intent document is verified for consistency and correctness in the treatment planning system. Similarly, "External structures" verifies the integrity and consistency of variables linked to the presence of immobilization devices, medical devices and prostheses in the Documents module and treatment planning system.

Regarding dose calculation, "Beam Configuration" verifies the correctness of variables describing the ionizing radiation beams that are used to target the tumor and from which the radiation dose distribution is calculated. "Dose Calculation" verifies the integrity of variables describing the dose calculation algorithm and associated parameters. "DVH and 3D Dose Distribution" verifies parameters describing the quality of the radiation dose distribution and the dose volume histogram calculated by the treatment planning system.

An independent verification of the accuracy of the dose distribution calculated by the treatment planning system is required. "Independent MU Calculation" verifies the integrity and consistency of the variables used to perform the independent MU calculation. An independent physical measurement of the planned radiation dose may also be required to ensure that the calculated radiation distribution is deliverable on the treatment machine. "Patient Specific QA" verifies that the output of the measurement is within tolerance. Note that for 3D photon plans, "Patient Specific QA" is not required. Once the planning of the treatment is completed in the treatment planning system, the treatment plan is transferred to the record and verify system. "Record and Verify" also contains treatment imaging instructions and patient scheduling information. This subprocess verifies that the information in the record and verify system is correct and consistent with that in the treatment planning system and documents module.

3.3 Variable Interactions

The specified variable relationships were determined from domain expertise, clinical practice, standardized practices in the field, the software modules used, physical characteristics of the treatment machines, imaging used and the physics of radiation dose calculation and treatment planning. For example, the prescription dose, which is the radiation treatment dose prescribed by the physician, is defined by the treatment site, intent of the treatment, dose per fraction and number of fractions among other variables. Furthermore, the prescription dose should be consistent across modules. In this case, assuming that patient manager (PM) is the module containing documents in a patient's chart and planning intent is the name of the document containing the prescription, an example of a causal dependency is *PrescriptionDose_PM_PlanningIntent* is dependent on *TreatmentSite_PM_PlanningIntent*, *CourseIntent_PM_PlanningIntent*, *DosePerFraction_PM_PlanningInten* and *NumberOfFractions_PM_PlanningIntent*. The naming of these variables reflects the module (PM) and document, planning intent (PI), within that module.

To reflect consistency of variable values across the modules representing the treatment planning system (TPS) and record and verify system (RV), *PrescriptionDose_TPS PrescriptionDose_RV* are said to be

dependent on *PrescriptionDose_PM_PlanningIntent*. An inconsistency arises when these variables have different values.

A conflict arises when the value of one variable precludes the value of another variable. An example of conflicting values of two variables is IMRT as the treatment modality and a 3D dose calculation point. A treatment modality of IMRT precludes the possibility of the dose calculation point being specified in 3D.

3.4 Graph Model of TPCR

The directed graph constructed from the relationships defined on all 346 variables is shown in Fig. 5. The graph contained a total of 553 direct dependencies. The vertices are color coded by the relative order of the subprocesses they belong to as shown in Fig. 4. Blue represents vertices belonging to subprocesses that occur early on the the TPCR and red represents vertices belonging to subprocesses that are visited towards the end of the TPCR. As illustrated, directed edges between the vertices indicate the direction of causality of the relationship between variables. The source and impact of an inconsistency at the first level are given by the predecessors and successors of the variables, as illustrated in Fig. 5. In this example, for vertex V_i, $\lambda_i^{in} = 1$ and $\lambda_i^{out} = 3$. The graph allows us to visualize the relative relationship between vertices within and across subprocesses.

A subset of the TPCR graph on a selection of variables is illustrated in Fig. 6. The direct predecessor vertices from the edges leading to *DoseFractionationType_PM_PlanningIntent* (V_{206}), indicate that it is directly dependent on *CourseIntent_PM_PlanningIntent* (V_{77}), *TreatmentSite_PM_PlanningIntent* (V_{73}), *RadiationType_PM_ PlanningIntent* (V_{207}) and *TreatmentModality_PM_PlanningIntent* (V_{80}). Similarly, the direct successor vertices, as determined from the edges leading away from (V_{206}), indicate that it impacts *PrescriptionDose_PM_PlanningIntent* (V_{212}), *DosePerFraction_PM_PlanningIntent*, (V_{218}), *NumberOfFractions_PM_PlanningIntent* (V_{221}).

3.5 Degree of Connection

Variables with the highest outconnection degrees along with their inconnection degree and the modules and subprocesses they belong to are listed in Table 1. The list of variables illustrates the high importance associated with variables contained in the planning instructions and imaging instructions, which are entered by the physician at the start of treatment planning, as these determine the contents of the patient's chart and treatment plan. Although not listed in the table, the prescription dose entered by the physician in the planning instructions document had an outconnection degree of 77. Note that variables with a still high, but lower impact score than those listed in Table 1, such as prescription dose, may have a high severity score, indicating that an error in these variables pose a high risk to the patient.

Variables with high inconnection degrees included the chart treatment approval status, GTV, PTV and CTV coverage, beam dose, beam MU and wedge parameters and appear in the later subprocesses listed in Fig. 4 including in Chart Treat Approved, Record and Verify, DVH and 3D Dose Distribution and Dose Calculation. These are affected by the variables entered in the initial stages of the treatment planning process including the variables listed in Table 1.

3.6 Constraint Specification

The finite set of variables, $\mathbf{V}$, each take an allowed set of values in a domain D. For the example defined below in the "Planning Intent and Dose Prescription" subprocess addressing a subset of 10 of the 346 variables , let $\mathbf{V} = \{$*TreatmentSite_PM_PlanningIntent*, *CourseIntent_PM_PlanningIntent*, *TreatmentModality_PM_PlanningIntent*, *DoseFractionationType_PM_PlanningIntent*, *RadiationType_PM _PlanningIntent*, *DosePerFraction_PM_PlanningIntent*, *NumberOfFractions_PM_PlanningIntent*, *PrescriptionDose_PM_PlanningIntent*, *PrescriptionDose_TPS*, *PrescriptionDose_RV*$\}$.

For each variable, V_i, we then defined a set D_i of permissible values. For instance, for the given subset of variables, the following allowable values were defined for select treatment sites:

$$\begin{aligned}
TreatmentSite_PM_PlanningIntent &\in \{Brain, Brain\,LGG, Brain\,HGG, Lung\,NSCLC\} \\
CourseIntent_PM_PlanningIntent &\in \{Curative, Palliative\} \\
TreatmentModality_PM_PlanningIntent &\in \{3D, IMRT\} \\
DoseFractionationType_PM_PlanningIntent &\in \{Conventional, Hypo\} \\
RadiationType_PM_PlanningIntent &\in \{Electrons, Photons\} \\
DosePerFraction_PM_PlanningIntent &\in \{180, 200, 300, 100\} \\
NumberOfFractions_PM_PlanningIntent &\in \{5, 10, 30, 33\} \\
PrescriptionDose_PM_PlanningIntent &\in \{3000, 5000, 5400, 5940, 6600\} \\
PrescriptionDose_TPS &\in \{3000, 5000, 5400, 5940, 6600\} \\
PrescriptionDose_RV &\in \{3000, 5000, 5400, 5940, 6600\},
\end{aligned}$$

where HGG stands for high grade glioma, LGG means low grade gliomas, NSCLC is non small cell lung carcinoma.

Subsequently, we defined the constraints, C_i. An example set of logical formulae that specify the constraints, C_8 related to V_8, that is prescription dose, is given below.

$$\begin{aligned}
PrescriptionDose_PM_PlanningIntent == DosePerFraction_PM_PlanningIntent \\
\times NumberOfFractions_PM_PlanningIntent \quad (1)
\end{aligned}$$

$$\{TreatmentSite\_PM\_PlanningIntent,\ CourseIntent\_PM\_PlanningIntent,$$
$$TreatmentModality\_PM\_PlanningIntent,\ DoseFractionationType\_PM\_PlanningIntent,$$
$$RadiationType\_PM\_PlanningIntent,\ DosePerFraction\_PM\_PlanningIntent,$$
$$NumberOfFractions\_PM\_PlanningIntent,\ PrescriptionDose\_PM\_PlanningIntent\}$$
$$\in \{(Brain, Palliative, 3D, Conventional, Photons, 300, 10, 3000),$$
$$(Brain\,LGG, Curative, IMRT, Conventional, Photons, 180, 30, 5400)$$
$$(Brain\,HGG, Curative, IMRT, Conventional, Photons, 180, 33, 5940)$$
$$(Lung\,NSCLC, Curative, IMRT, Conventional, Photons, 200, 33, 6600)$$
$$(Lung\,NSCLC, Curative, IMRT, Hypo, Photons, 1000, 5, 5000)\} \quad (2)$$

$$PrescriptionDose\_TPS == PrescriptionDose\_PM\_PlanningIntent \quad (3)$$

$$PrescriptionDose\_RV == PrescriptionDose\_PM\_PlanningIntent \quad (4)$$

3.7 Automated TPCR Review

Inconsistencies are detected automatically by solving for constraint violation in the values of the variables. After execution, the program lists the status of the subprocesses as shown in Fig. 7. Here, there is an error in the treatment modality and the need for IMRT QA. A tick next to a subprocess indicates that no inconsistencies were found in that subprocess and all variables were correct. A cross indicates the presence of inconsistent variables. The user can navigate through the listed subprocesses by clicking on them. Clicking on a subprocess will list the variables belonging to that subprocess and their value in an adjacent window. As with the subprocesses, the automated chart review program indicates the status of

the evaluation of the variables through ticks and crosses. The possible source of an inconsistency for a given variable is found by clicking on that variable. Parent variables with level 1 are directly connected to the variable while variables at higher levels are indirectly connected with the degree of removal from the variable being examined increasing with level number. The impact of an error in a given variable on other variables in the treatment chart is found by clicking on that variable and examining the children variables and their level.

Once the inconsistencies have been detected, the user has an option to generate a report describing the output of the program as shown in Figs. 8 and 9. If the plan is not approved, the report states the number of constraints violated and the number of variables in the RT chart which were found to be inconsistent, according to the relationships and constraints described. The first table gives a summary of the errors, or inconsistencies, detected by the automated chart review program, their impact and severity. Each inconsistency detected and the contextual information associated with the inconsistency is reported in a second table. The third table lists the module and subprocess that the variables belong to along with the impact, defined by the outconnection degree, and severity of each inconsistency. For instance, in this example, IMRT QA has a value of Yes and belongs to Module Patient Manager and Subprocess Patient Specific QA. This information is required in order for the user to know where to correct an error, if present, and to decide in which order to investigate and correct the detected inconsistencies. For instance, they may wish to first investigate and correct variables with a high outconnection degree and high severity score. The cumulative effect of the outconnection degree and severity associated with the different inconsistencies are provided to the user as pareto charts as shown in Fig. 9.

Finally, once all variables in all subprocesses have been evaluated and if no inconsistencies are detected, the treatment plan is approved for treatment and delivered on the treatment machine.

4 Discussion

We have presented a comprehensive graph-based model of the TPCR process that can be used for risk assessment and the development of an automated pretreatment physics chart solution. The model integrates information about the underlying structure of the TPCR process across all software modalities being checked. The automated chart review solution combines a modular approach, graph theory and constraint programming to detect inconsistencies in a patient's chart, the source of the inconsistencies and how they propagate. Impact scores, quantify the effect of an inconsistency on other variables based on vertex connection analysis, and predefined severity scores assess the tolerability of the inconsistency. Such an automated solution can be used for risk assessment, error detection and as a guide for error correction in the TPCR. It may also improve the reliability of the chart review process by reducing the risk of human error associated with manual checks and by serving as a training tool for the chart reviewer.

The grouping and logical flow of the checks to be performed on the variables was represented by subprocesses in a flowchart mapping all steps in the TPCR from document verification to verification of the dose calculation parameters to verification of the parameters in the record and verify system. We sought to make our solution vendor agnostic but comprehensive by including key variables that ought to be checked as part of a pretreatment physics chart review. The severity scales proposed for the different inconsistencies may be further refined according to guidelines provided by Ford et al. [17] and AAPM Task Group 100 [18].

Capturing the relationship between all variables in the TPCR process was of foremost importance in defining a solution for the automated TPCR. The relationships and constraints are based on domain knowledge, the general principles of radiation physics, recommendations from AAPM Task Groups 40 and 275 [19, 1] and clinical practice. We chose to integrate a predefined model of the relationship between variables in the TPCR process into the solution as the relationships are known in advance and are deterministic. Modeling the relationships between the variables resulted in a comprehensive solution that does not require prior data and can be validated to ensure it meets clinical specifications for the TPCR.

Such a model also promotes standardization. Our solution differs from existing automated solutions in the literature for the TPCR that do not provide contextual information about errors or recent Bayesian network based methods where probabilistic relationships among a subset of variables are learnt from prior treatment plans [20, 21, 22].

While the relationships and constraints are currently entered manually, we plan to extend our solution to automatically determine constraints from standardized document templates, the treatment planning system parameters and the linear accelerator characteristics. Such capability will also facilitate redefinition of the constraints if new treatment paradigms and technologies are implemented.

As described in the Results section, the model for the TPCR process comprised 5 modules, 19 subprocesses and 346 variables of which 225 were distinct. The large number of variables and subprocesses in the solution is an indication of the complexity of the TPCR process. The modular approach in this study facilitates formulation of the dependencies between variables and formalization of the problem. We found it useful to first make a list of individual items to be checked followed by the modules in which they appear, the subprocesses where they are checked, their types and allowed values before subsequently formulating the dependencies between them and constraints.

An undirected graph, as opposed to a directed graph, while useful for capturing variable dependencies, does not permit modeling of the causality of the dependencies. Since an individual item, for instance prescription dose, may appear in multiple modules, for example, in the treatment planning system and record and verify systems, thus yielding multiple variables. The independent variable in this case is the instance of the item where its value is first specified or generated, for example, in the planning directive. Instances where the item is replicated, such as in the treatment planning system for prescription dose, are considered to be dependent on the parent variable.

When ranked in order of outconnection degree, patient MRN and variables contained in the planning intent had the highest outconnection degree and therefore the highest impact on other variables emphasizing the need to ensure these variables are correct at the very beginning of the chart review, as is usually the

case in clinical practice. Thus, the solution presented here does not only detect errors, but may also help improve the efficiency of error correction by providing advanced warning to the user of the location in the TPCR process of the inconsistency and the number and manner in which other related variables are affected.

We note that the concepts presented in this study are generally applicable to any chart review process. The proposed solution is amenable to customization and extension for the inclusion of new variables and is adaptable to variations in the variables used, modules, subprocesses and types of checks performed according to treatment site and clinical practice or as described in TG 275 [1].

A key recommendation of AAPM Task Group 275 [1] is that the TPCR should be based on risk analysis methods such as process maps and FMEA. The combination of information on the source, impact and severity of an inconsistency allows us to assess the risk posed by a given error. The dependency information obtained from the graph is useful towards a failure modes and effects analysis (FMEA) [18, 12] of the TPCR process or error pathway analysis as performed by Ezzel et al. on RO-ILS data [23] since it allows automatic identification of the cause and effect of an inconsistency at different degrees of connection and across different modules and subprocesses. In a conventional FMEA, such an in-depth and comprehensive capture of the TPCR process may be cumbersome and time consuming.

We expect that clinical use of our chart review solution will provide data on the frequency of different types of errors encountered as has been reported in other studies [24, 23, 12, 13]. This will permit subsequent data mining for a more complete risk assessment, and concomitant risk reduction [25]. This can take the form of a systematic review of where most errors are generated and training to reduce these errors.

Given the number of variables, modules and types of checks involved, the physics chart review can initially be challenging for the chart reviewer, particularly if they are new to the process. A potential application of our solution is as an education and training tool for performing the physics chart review in a structured and standardized manner in accordance with key recommendations in AAPM Task Group 275 [1]. It can also serve as a tool to enhance communication among the clinical care team. In addition

to helping the chart reviewer understand the underlying architecture of the TPCR process, the structured nature of our solution can be a useful guide regarding how to navigate the sequence of steps involved in a physics chart review.

Definition of the solution using graphs and constraint programming also lays the foundation for the use of advanced methods such as automated theorem provers in combination with first order logic to solve for inconsistencies. Such a solution would allow us to verify the correctness of the constraint specifications in addition to solving for inconsistencies and understanding the impact of additional checks introduced in the future [16, 26]. The methods proposed in this study are synergistic with ongoing efforts to improve clinical practice through modeling and automation [27, 28].

5 Conclusions

We have comprehensively modeled the TPCR process revealing it to be amenable to an automated solution for error detection, risk assessment and error tracking. Our TPCR solution identifies all errors or logical inconsistencies in a chart, as defined by the specifications of the TPCR, their source, severity and how they propagate. This contextual information is useful for risk assessment and error correction. The solution presented may help reduce or eliminate human error in the TPCR process, thus reducing the risk of a faulty radiation plan being delivered.

6 Disclosures

The authors have no conflicts to disclose.

Bibliography

[1] E. Ford, L. Conroy, L. Dong, L. F. Los Santos, A. Greener, G. GweYa Kim, J. Johnson, P. Johnson, J. G. Mechalakos, B. Napolitano, S. Parker, D. Schofield, K. Smith, E. Yorke, and M. Wells, "Strategies for effective physics plan and chart review in radiation therapy: Report of AAPM Task Group 275," *Med. Phys.*, vol. 47, no. 6, pp. e236–e272, 2020.

[2] O. Gopan, J. Zeng, A. Novak, M. Nyflot, and E. Ford, "The effectiveness of pretreatment physics plan review for detecting errors in radiation therapy.," *Med Phys*, vol. 43, no. 9, pp. 5181–5187, 2016.

[3] IAEA, "Safety reporting and learning system for radiotherapy (safron)." https://rpop.iaea.org/RPOP/RPoP/Modules/login/saf ron-register.htm, 2017.

[4] L. M. Mazur, P. R. Mosaly, M. Jackson, S. X. Chang, K. D. Burkhardt, R. D. Adams, E. L. Jones, L. Hoyle, J. Xu, J. Rockwell, and L. B. Marks, "Quantitative assessment of workload and stressors in clinical radiation oncology.," *Int J Radiat Oncol Biol Phys*, vol. 83, no. 5, pp. e571–576, 2012.

[5] R. A. Siochi, E. C. Pennington, T. J. Waldron, and J. E. Bayouth, "Radiation therapy plan checks in a paperless clinic," *Journal of Applied Clinical Medical Physics*, vol. 10, no. 1, pp. 43–62, 2009.

[6] E. E. Furhang, J. Dolan, J. K. Sillanpaa, and L. B. Harrison, "Automating the initial physics chart-checking process," *Journal of Applied Clinical Medical Physics*, vol. 10, no. 1, pp. 129–135, 2009.

[7] J. Xia, C. Mart, and J. Bayouth, "A computer aided treatment event recognition system in radiation therapy: Error detection in radiation therapy," *Med. Phys.*, vol. 41, no. 1, pp. 011713–1–011713–6, 2013.

[8] T. Halabi and H.-M. Lu, "Automating checks of plan check automation.," *J Appl Clin Med Phys*, vol. 15, no. 4, pp. 4889–4897, 2014.

[9] J. M. Dewhurst, M. Lowe, M. J. Hardy, C. J. Boylan, P. Whitehurst, and C. G. Rowbottom, "AutoLock: a semiautomated system for radiotherapy treatment plan quality control.," *J Appl Clin Med Phys*, vol. 16, no. 3, p. 5396, 2015.

[10] E. L. Covington, X. Chen, K. C. Younge, C. Lee, M. M. Matuszak, M. L. Kessler, W. Keranen, E. Acosta, A. M. Dougherty, S. E. Filpansick, and J. M. Moran, "Improving treatment plan evaluation with automation.," *J Appl Clin Med Phys*, vol. 17, no. 6, pp. 16–31, 2016.

[11] C. Holdsworth, J. Kukluk, C. Molodowitch, M. Czerminska, C. Hancox, R. A. Cormack, K. Beaudette, and J. H. Killoran, "Computerized System for Safety Verification of External Beam Radiation Therapy Planning.," *Int J Radiat Oncol Biol Phys*, vol. 98, no. 3, pp. 691–698, 2017.

[12] S. Liu, K. K. Bush, J. Bertini, Y. Fu, J. M. Lewis, D. J. Pham, Y. Yang, T. R. Niedermayr, L. Skinner, L. Xing, B. M. Beadle, A. Hsu, and N. Kovalchuk, "Optimizing efficiency and safety in external beam radiotherapy using automated plan check (APC) tool and six sigma methodology.," *J Appl Clin Med Phys*, vol. 20, no. 8, pp. 56–64, 2019.

[13] S. L. Berry, Y. Zhou, H. Pham, S. Elguindi, J. G. Mechalakos, and M. Hunt, "Efficiency and safety increases after the implementation of a multiinstitutional automated plan check tool at our institution," *J Appl Clin Med Phys*, vol. 21, no. 4, pp. 51–58, 2020.

[14] P. Xia, D. LaHurd, P. Qi, A. Mastroianni, D. Lee, A. Magnelli, E. Murray, M. Kolar, B. Guo, T. Meier, S. T. Chao, J. H. Suh, and N. Yu, "Combining automatic plan integrity check (APIC) with standard plan document and checklist method to reduce errors in treatment planning.," *J Appl Clin Med Phys*, pp. 124–133, 2020.

[15] M. Rausand, *Risk assessment: theory, methods, and applications*. Statistics in practice, Hoboken, N.J: Wiley, 2011.

[16] R. Munbodh, H. P. Zaveri, M. B. Caminati, and J. K. Bowles, "Formalization and automation of quality assurance processes in radiation oncology," *Med. Phys.*, vol. 45, no. 6, p. e274, 2018.

[17] E. C. Ford and S. B. Evans, "Incident learning in radiation oncology: A review," *Med. Phys.*, vol. 45, no. 5, pp. e100–e119, 2018.

[18] M. S. Huq, B. A. Fraass, P. B. Dunscombe, J. P. Gibbons, G. S. Ibbott, A. J. Mundt, S. Mutic, J. R. Palta, F. Rath, B. R. Thomadsen, J. F. Williamson, and E. D. Yorke, "The report of Task Group 100

of the AAPM: Application of risk analysis methods to radiation therapy quality management: TG 100 report," *Med. Phys.*, vol. 43, no. 7, pp. 4209–4262, 2016.

[19] G. J. Kutcher, L. Coia, M. Gillin, W. F. Hanson, S. Leibel, R. J. Morton, J. R. Palta, J. A. Purdy, L. E. Reinstein, G. K. Svensson, M. Weller, and L. Wingfield, "Comprehensive QA for Radiation Oncology," tech. rep., AAPM, 1994.

[20] A. M. Kalet, J. H. Gennari, E. C. Ford, and M. H. Phillips, "Bayesian network models for error detection in radiotherapy plans," *Phys. Med. Biol.*, vol. 60, no. 7, pp. 2735–2749, 2015.

[21] S. M. H. Luk, J. Meyer, L. A. Young, N. Cao, E. C. Ford, M. H. Phillips, and A. M. Kalet, "Characterization of a Bayesian networkbased radiotherapy plan verification model," *Med. Phys.*, vol. 46, no. 5, pp. 2006–2014, 2019.

[22] X. Chang, H. H. Li, A. M. Kalet, and D. Yang, "Development and Validation of a Bayesian Network Method to Detect External Beam Radiation Therapy Physician Order Errors," *International Journal of Radiation Oncology*Biology*Physics*, vol. 105, no. 2, pp. 423–431, 2019.

[23] G. Ezzell, B. Chera, A. Dicker, E. Ford, L. Potters, L. Santanam, and S. Weintraub, "Common error pathways seen in the RO-ILS data that demonstrate opportunities for improving treatment safety," *Practical Radiation Oncology*, vol. 8, no. 2, pp. 123–132, 2018.

[24] T. Halabi, H.-M. Lu, D. A. Bernard, J. C. H. Chu, M. C. Kirk, R. J. Hamilton, Y. Lei, and J. Driewer, "Automated survey of 8000 plan checks at eight facilities.," *Med Phys*, vol. 43, no. 9, pp. 4966–4972, 2016.

[25] P. E. Gabriel, K. D. Woodhouse, A. Lin, J. C. Finlay, R. B. Young, E. Volz, S. M. Hahn, J. M. Metz, and A. Maity, "An automated electronic system for managing radiation treatment plan peer review reduces missed reviews at a large, high-volume academic center," *Practical Radiation Oncology*, vol. 6, no. 6, pp. e307–e314, 2016.

[26] J. K. Bowles and R. Munbodh, "Computer aided verification of radiotherapy treatment plans," *Med. Phys.*, vol. 46, no. 6, p. e195, 2019.

[27] R. Munbodh, T. M. Roth, K. L. Leonard, J. Brindle, and E. E. Klein, "Real-time analysis and display of quantitative measures to track and improve clinical workflow," *Med. Phys.*, vol. 46, no. 6, p. e197, 2019.

[28] R. Munbodh, K. Leonard, T. Roth, M. Schwer, J. Brindle, and E. Klein, "A data-driven analytical framework to track and improve clinical workflow in radiation oncology," *Med. Phys.*, vol. 47, no. 6, p. e566, 2020.

Figure 1: The customary workflow for EBRT consists of prescription of the radiation dose by the physician, acquisition of a diagnostic energy planning CT by a therapist, creation of a patient-specific treatment plan by a dosimetrist to deliver the prescribed dose, review and approval of the treatment plan by the physician, review and approval of the treatment plan (TPCR) by a medical physicist, delivery of the treatment plan to the patient and, finally, verification of the correctness of the delivered dose

Figure 2: The flowchart displays the different steps required to formalize the TPCR process.

Figure 3: The flowchart illustrates the steps in the automated chart review process. Variables can either be checked simultaneously or sequentially depending on the order in which the subprocesses are visited during the TPCR. The severity of a logical inconsistency is defined by a preassigned score and its impact by its outconnection degree as determined from the directed graph.

Figure 4: We modeled the TPCR as being composed of 19 subprocesses. The activity diagram illustrates the subprocesses and the sequence in which they appear in the TPCR.

Figure 5: The vertices are coded by the color of the subprocess to which they belong, with a transition from blue to red as we proceed from the first to the last subprocess in the TPCR. Blue verices tend to be clustered in the center and have a high outconnection degree while red vertices tend to be on the periphery of the graph. A vertex, V_i, and its predecessor and successor vertices at level 1 are shown.

Figure 6: The figure shows a subset of the TPCR graph. In this graph, V_{77} is a predecessor to V_{206} indicating that it directly influences the latter and V_{212} is a successor to V_{206} indicating that it is directly influenced by V_{206}.

Figure 7: The status of the subprocesses and variables checked are indicated by ticks and crosses with a cross indicating inconsistency. The parents and children of an inconsistent variable, and therefore its source and impact, are listed by clicking on the affected variable. The numbers next to the parent and children indicate their level, that is, how far removed they are from the inconsistent variable.

Figure 8: The report lists the constraints violated, inconsistent variables, the modules and subprocess the variables belong to, the impact of the inconsistency on other variables, as determined from the outconnection degree, and severity of an error associated with the variables.

Figure 9: (a) Pareto chart calculated from outconnection. Inconsistent variables are graphed in descending order of outconnection degree (impact). The line shows the cumulative outconnection degree summed over the inconsistent variables. (b) Pareto chart calculated from severity of error. The line shows the cumulative effect of the inconsistencies in terms of severity associated with a variable.

Table 1: Variables with the highest outconnection degree.

No.	Variable	Variable Name	ζ_i^{out}	ζ_i^{in}	Module	Subprocess
1	V14	Patient MRN	286	0	Patient Manager	1
2	V54	Planning Intent Present	250	0	Patient Manager	3
3	V55	Planning Intent Approved	249	1	Patient Manager	3
4	V49	Diagnosis Code	243	1	Patient Manager	1
5	V73	Treatment Site	239	4	Patient Manager, Planning Intent	3
6	V77	Course Intent	188	4	Patient Manager, Planning Intent	3
7	V207	Radiation Type	185	7	Patient Manager, Planning Intent	3
8	V80	Treatment Modality	185	7	Patient Manager, Planning Intent	3
9	V84	CT Required	143	7	Patient Manager, Planning Intent	5
10	V86	CT Present	136	8	Treatment Planning System	5
11	V96	4D CT Required	133	8	Patient Manager, Simulation Instructions	5
12	V91	Patient Orientation	129	8	Patient Manager, Simulation Instructions	5
13	V113	PET CT Required	128	8	Patient Manager, Simulation Instructions	5
14	V109	MRI Required	128	9	Patient Manager, Simulation Instructions	5
15	V103	4D CT Present	127	9	Treatment Planning System	5
16	V114	PET CT Present	127	9	Patient Manager, Simulation Instructions	5
17	V110	MRI Present	126	5	Treatment Planning System	5
18	V147	PTV Present	126	10	Patient Manager, Simulation Instructions	3
19	V115	MRI Registered to CT	126	12	Treatment Planning System	5
20	V111	4D CT Extent	126	9	Patient Manager, Simulation Instructions	5
21	V100	4D CT Number of Phases	126	9	Patient Manager, Simulation Instructions	5
22	V97	CT Artefacts Present	126	2	Treatment Planning System	5
23	V94	CT Extent	126	6	Patient Manager, Simulation Instructions	5
24	V88	PET CT Integrity Approved	126	11	Treatment Planning System	5
25	V116	MRI Integrity Approved	125	13	Treatment Planning System	5

Variables pertaining to patient identifiers and the planning and imaging instructions entered by the physician had the highest outconnection degrees and impacted the most variables in the TPCR process. Subprocess 1 = Patient Information and Plan Status, 2 = Presence of Primary Treatment Related and Physics Documents, 3 = Planning Intent and Dose Prescription, 5 = Imaging Integrity.

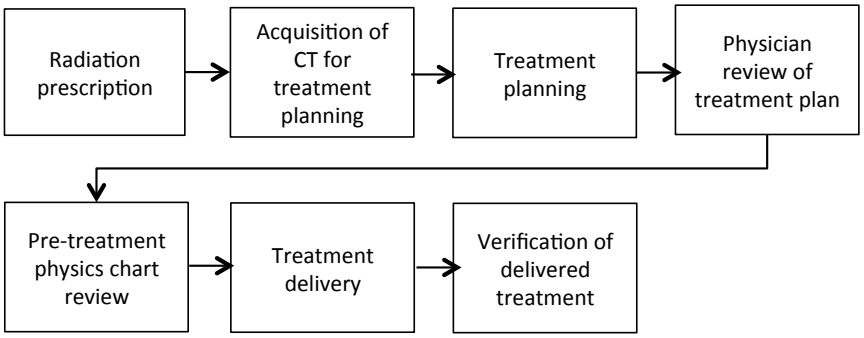

Fig. 1: Steps in radiation therapy planning.

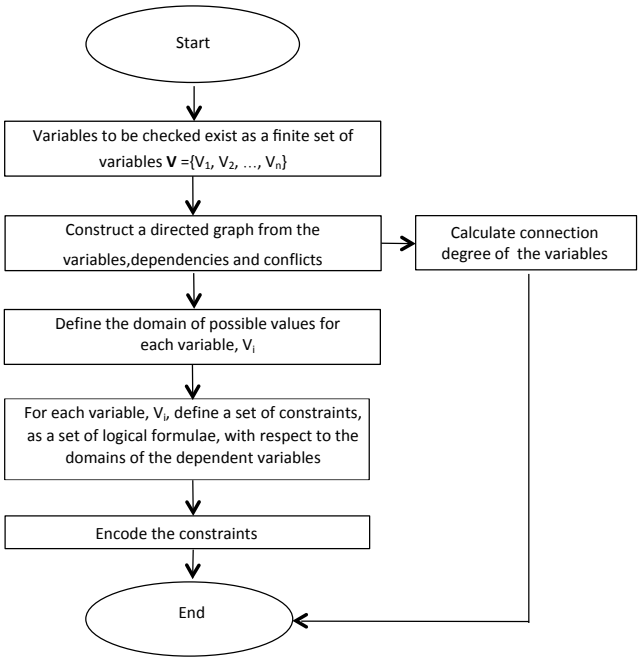

Fig. 2: Formalization of TPCR process.

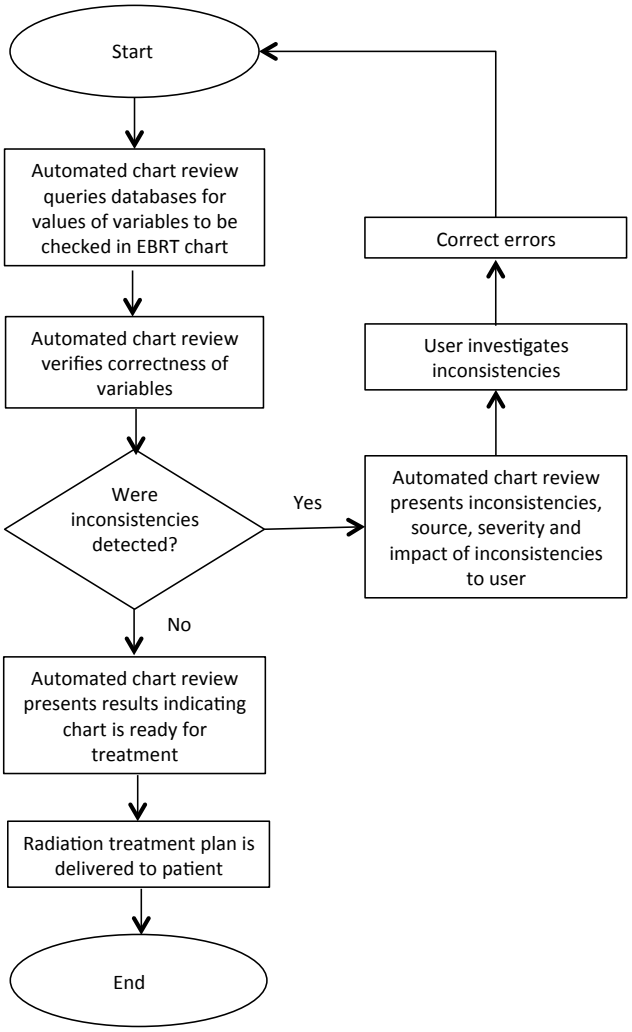

Fig. 3: Chart review process.

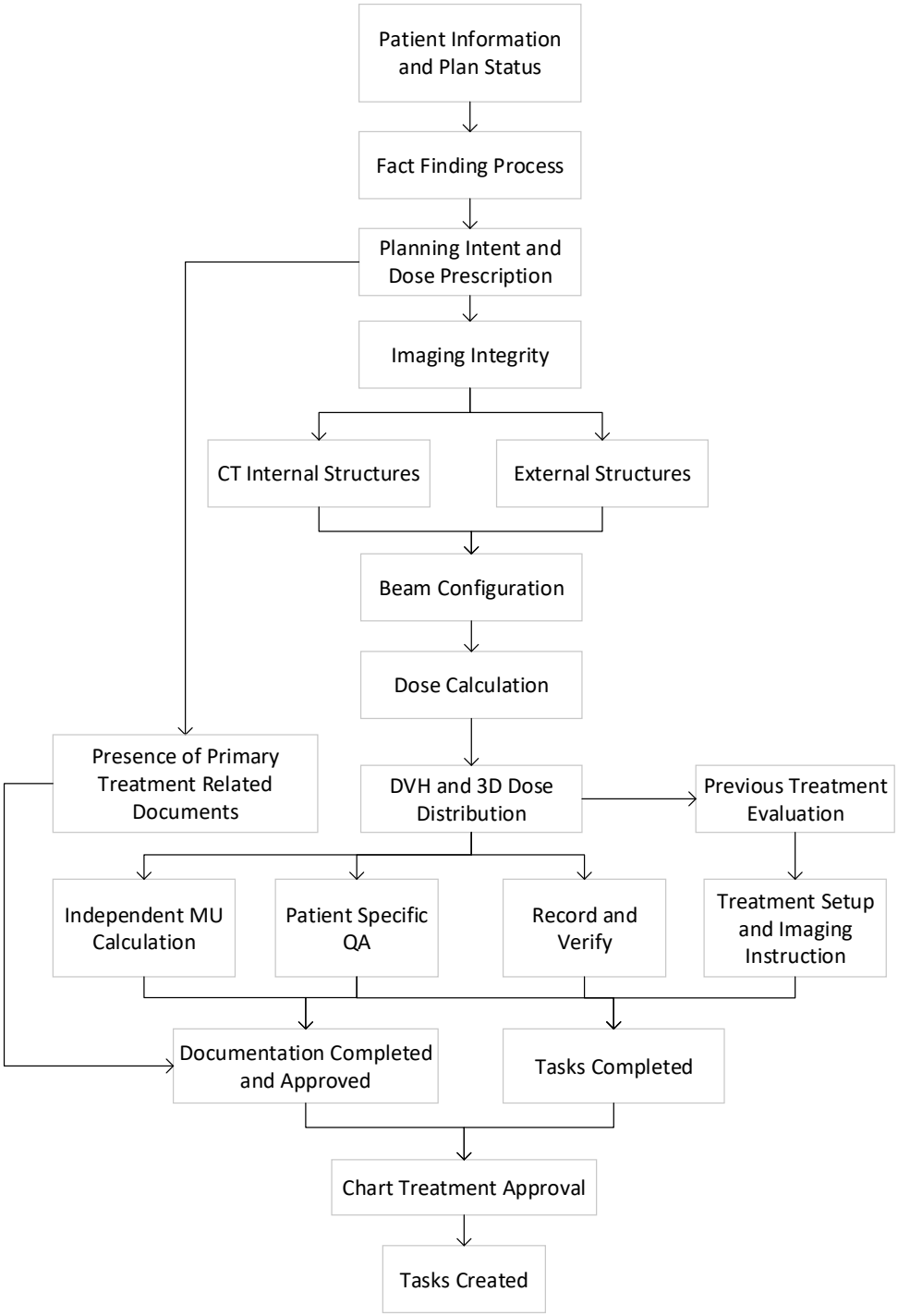

Fig. 4: Activity diagram of subprocesses in the TPCR.

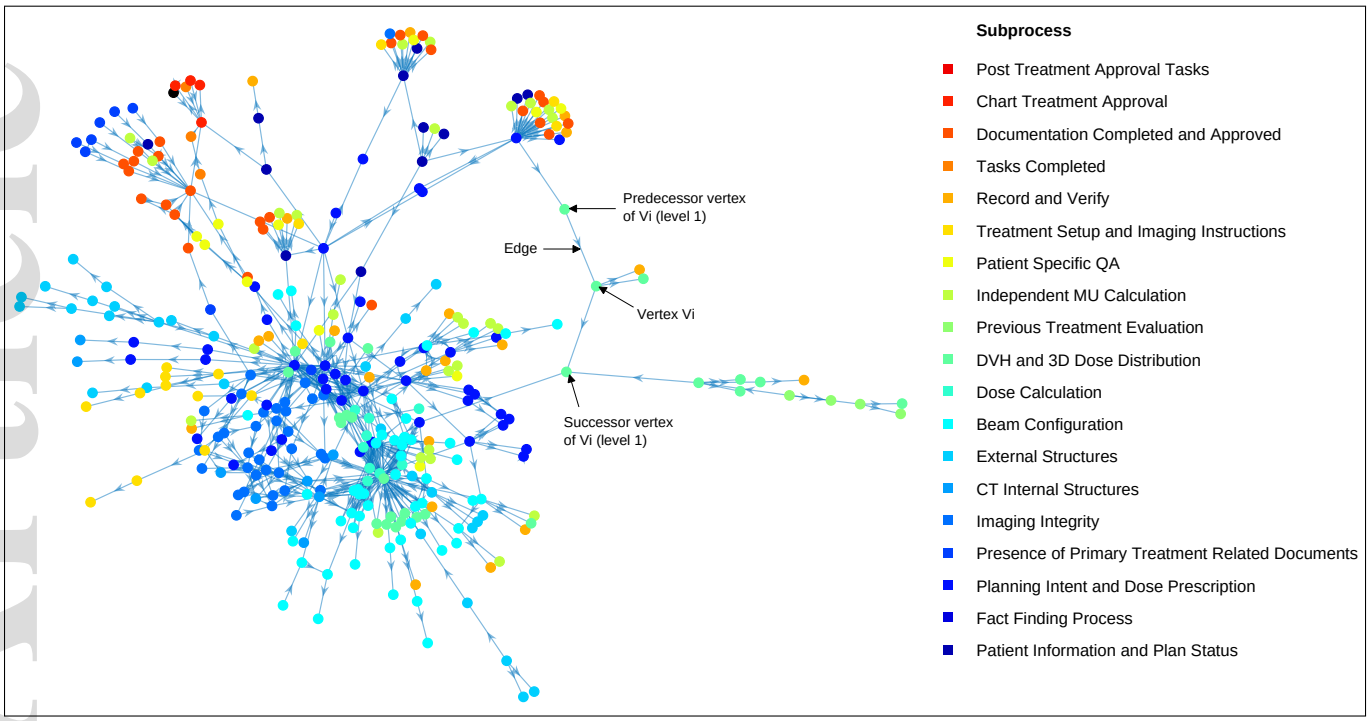

Fig. 5: An illustration of the graph model of the TPCR.

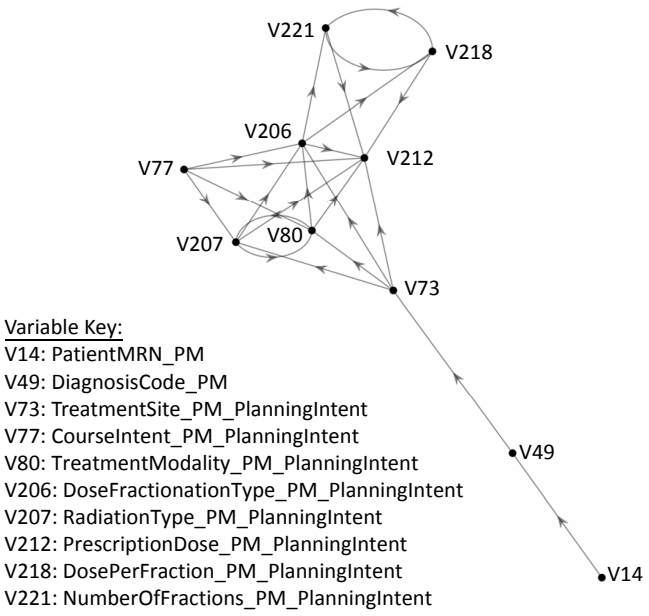

Fig. 6: Graph of subset of variables.

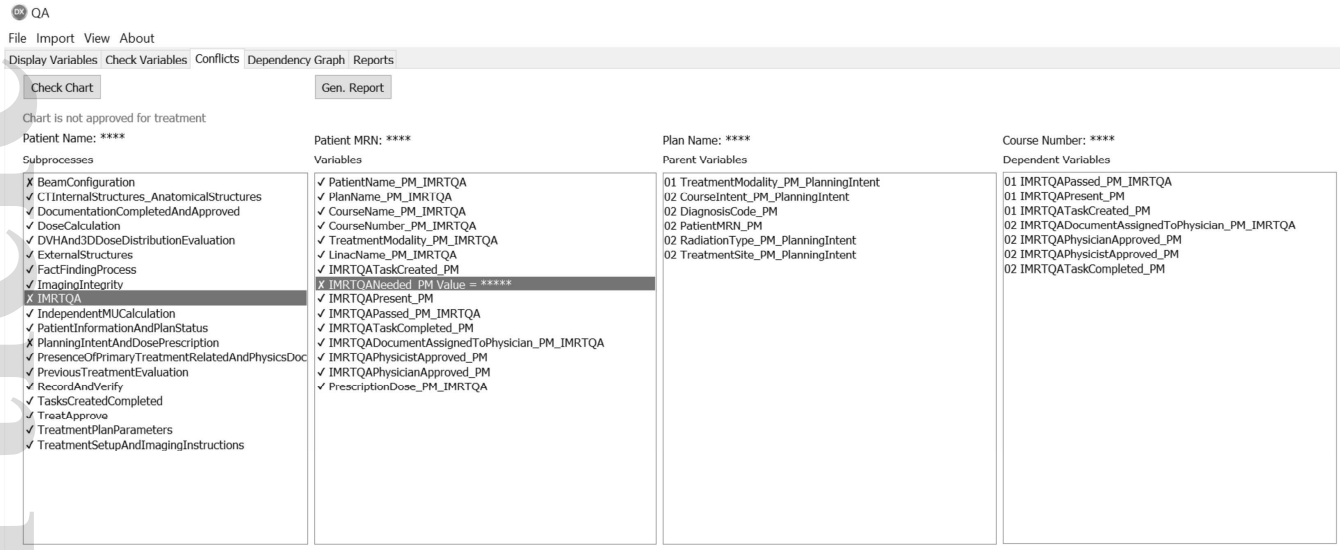

Fig. 7: Navigation of Results.

Automated Chart Review Report

Patient name: xxx
Patient MRN: xxx
Plan name: xxx
Course number: xx
Date: mm/dd/yyyy

Chart Review
Treatment plan is not approved for treatment
Number of constraints violated: 4
Number of inconsistent variables: 6
Cumulative impact score: 510
Cumulative severity score: 11

	Conflict
1	IMRTQANeeded_PM, TreatmentModality_PM_PlanningIntent
2	DoseRate_TPS is invalid
3	DoseRate_TPS, DoseFractionationType_PM_PlanningIntent
4	PrescriptionDose_PM, PrescriptionDose_TPS

Variable	Value	Module	Sub-process	Out Connectivity	Severity
Treatment modality	3D	Patient Manager	Planning Intent and Dose Prescription	185	2
Dose fractionation type	Conventional	Patient Manager	Planning Intent and Dose Prescription	124	2
Prescription dose	54	Patient Manager	Planning Intent and Dose Prescription	77	2
Prescription dose	50	Treatment Planning System	Planning Intent and Dose Prescription	58	2
Dose rate	1000	Treatment Planning System	Beam Configuration	53	2
IMRT QA needed	Yes	Patient Manager	Patient Specific QA	13	1

0 = Warning, 1 = Needs attention but user can proceed with other corrections simultaneously,
2 = Hard stop, needs immediate attention

Fig. 8: Error report generated by automated chart review program.

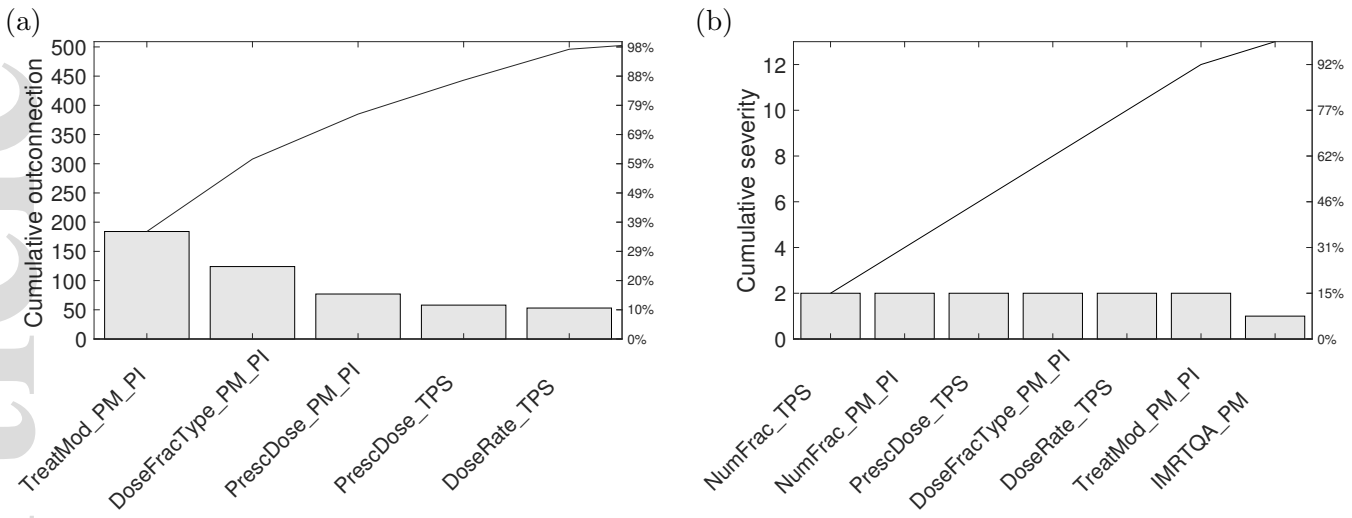

Fig. 9: Pareto charts of outconnection degree and severity.